A Twisted Cucurbit[14]uril-based Fluorescent Supramolecular Polymer Mediated by Metal Ion

Yang Luo [a], *Wei Zhang* [a], *Mao Xia Yang* [a], *Xian Hao Feng* [a], *Carl Redshaw* [b], *Qing Li* [a], *Zhu Tao* [a], *Xin Xiao* [a*]

[a] Key Laboratory of Macrocyclic and Supramolecular Chemistry of Guizhou Province, Guizhou University, Guiyang 550025, China

[b] Department of Chemistry, University of Hull, Hull HU6 7RX, U. K.

Keywords: Twisted curcubit[14]uril, supramolecular polymer, coordination interaction, Ni^{2+}.

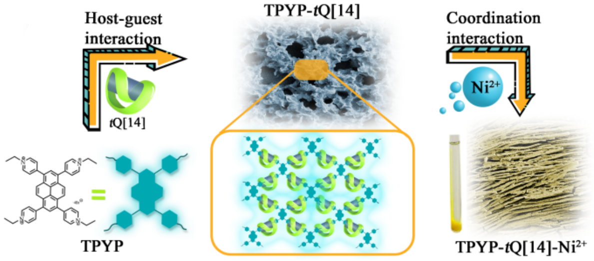

Abstract

Twisted cucurbit[14]uril, *t*Q[14], forms a fluorescent supramolecular polymer with the water-soluble fluorescent tetrapyridinium pyrene compound TPYP via host-guest interactions. Binding is via the alkyl chains and pyridines of TPYP at a molar ratio of 2:1 (*t*Q[14]:TPYP) and the structure forms a loose and porous supramolecular polymer TPYP-*t*Q[14]. On addition of different metals to a solution of TPYP-*t*Q[14], it was found that Ni^{2+} significantly reduced the emission of TPYP-*t*Q[14], and impacted the morphology of the TPYP-*t*Q[14], changing it from a loose porous structure to a chain. Due to the special structure of *t*Q[14], the mechanism of regulation is considered to be a coordination interaction between Ni^{2+} and the third portal of *t*Q[14]. This research makes full use of the structural advantages associated with twisted cucurbit[*n*]urils, and provides a new method for controlling the structure of a polymer through coordination-type interactions.

Introduction

Twisted cucurbit[14]uril (*t*Q[14], Scheme 1) which consists of 14 glycoluril-$(CH_2)_2$- units with a 360° twist was first discovered and reported by Tao *et al.* in 2013 [1]. *T*Q[14] has a number of unique structural characteristics that are quite different from ordinary cucurbit[*n*]urils (Q[*n*], n=5-8, 10). For example, it has three metal coordination sites and two unique cavities with a larger size than those of Q[5, 6], but smaller than those of Q[7, 8]. The high degree of polymerization exhibited by *t*Q[14] results in the extremely low yield [2, 3], and so research on this system is scant [4-9]. Indeed, research on *t*Q[14] to-date mainly features the work by Zhang and co-workers [4,5], who constructed a series of amino acid complexes incorporating *t*Q[14] and a stimuli-responsive supramolecular assembly by *t*Q[14] and thioflavin T. In addition, Li and co-workers [5,7] reported the interactions of *t*Q[14] with bipyridine derivatives and observed a series of long-chain amine-containing molecules. Thus, the study of twisted cucurbit[*n*]uril is still at an embryonic stage, and has mainly focused on the nature of *t*Q[14] and exploration of its host-guest chemistry. These studies provide us with some precious information about the structure and cavity properties of *t*Q[14], and based on these reports, our group first [9] constructed a network-like supramolecular polymer based on *t*Q[14] and a porphyrin which utilized host-guest interactions.

Supramolecular polymer formation is driven by non-covalent interactions, such as hydrogen bonds, π-π interactions, host-guest interactions, etc. [10-14], and have been widely used in many fields, including in the emerging development of macrocyclic compounds [15-20]. In the area of Q[*n*] macrocycles, many scholars have made seminal contributions [16-18], for example, Zhang and co-workers [17] have constructed linear and weight-controllable supramolecular polymers by the strategy of self-sorting based on *nor-seco*-cucurbit[10]uril. Liu's group [18] have reported a linear and near-infrared supramolecular polymer based on Q[8] and anthracene derivatives for cell imaging and could transform its shape from linear into nanoparticles upon adding sulfonatocalix[4]arene. From the above, it is evident that cucurbiturils have unique advantages in the construction of flexible and controllable supramolecular polymers through the availability of non-covalent interactions.

In this work, a supramolecular polymer TPYP-*t*Q[14] is constructed via the host-guest interaction between *t*Q[14] with its unique double-cavities and a fluorescent water-soluble guest molecule TPYP (Scheme S1), the latter has been modified with four short ethane chains at the 1,3,6,8-tetra(pyridin-4-yl)pyrene core [21-27]. The *T*Q[14] binds with the pyridines and alkyl chains of the TPYP in a ratio of 2:1 (*t*Q[14]:TPYP), and extends around to form a loose and porous supramolecular polymer. Interestingly, following the addition of a variety of metal ions, it was found that in the presence of Ni^{2+}, TPYP-*t*Q[14] produced a yellow precipitate and the fluorescence of the TPYP-*t*Q[14]-Ni^{2+} was greatly reduced [28-30]. SEM and confocal microscopy both found that the addition of Ni^{2+} changed the original morphology of the TPYP-*t*Q[14] from a loose porous network supramolecular polymer to a polymer chain, which is largely attributed to the unique structure of *t*Q[14]. The two cavities of *t*Q[14] bind the TPYP through host-guest interactions, while the third portal of the *t*Q[14] coordinates with the Ni^{2+}, leading to the formation of a metal-mediated supramolecular polymer [31, 32] (Scheme 1).

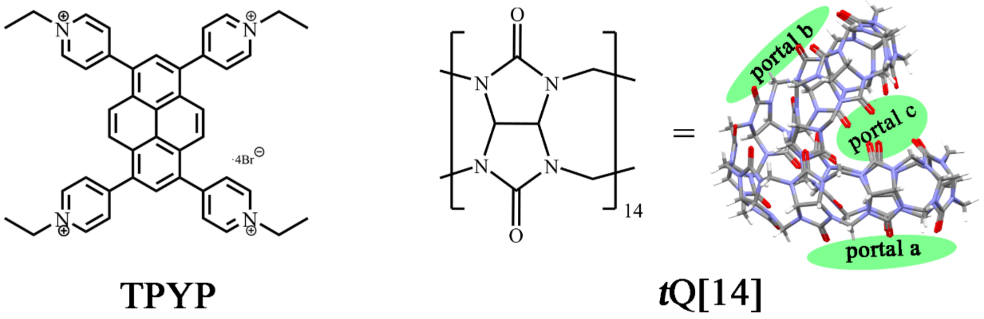

Scheme 1. Structures of **TPYP** and ***t*Q[14]**

Results and Discussion

^{1}H NMR spectroscopic titrations were used to study the host-guest interactions between the TPYP and *t*Q[14]. As shown in Figure 1, the shielding effect generated by the two hydrophobic cavities of *t*Q[14] causes the proton signals of pyridine and the methyl of TPYP to clearly shift to high field as an increasing amount of *t*Q[14] was added. In particular, the proton signal of pyridine (H$_c$) moves from δ= 8.99 to 8.82 ppm, and the signal of methyl (H$_a$) moves from δ=1.65 to 1.54 ppm, respectively. The signal peak associated with the methylene group (H$_b$) is completely masked by the solvent peak of water, but it can still be inferred that H$_b$ should be shifted to the high field like the proton signals of pyridine (H$_c$) and the methyl group (H$_a$). Thus, the alkyl chain and pyridine part of TPYP enter the cavity of *t*Q[14].

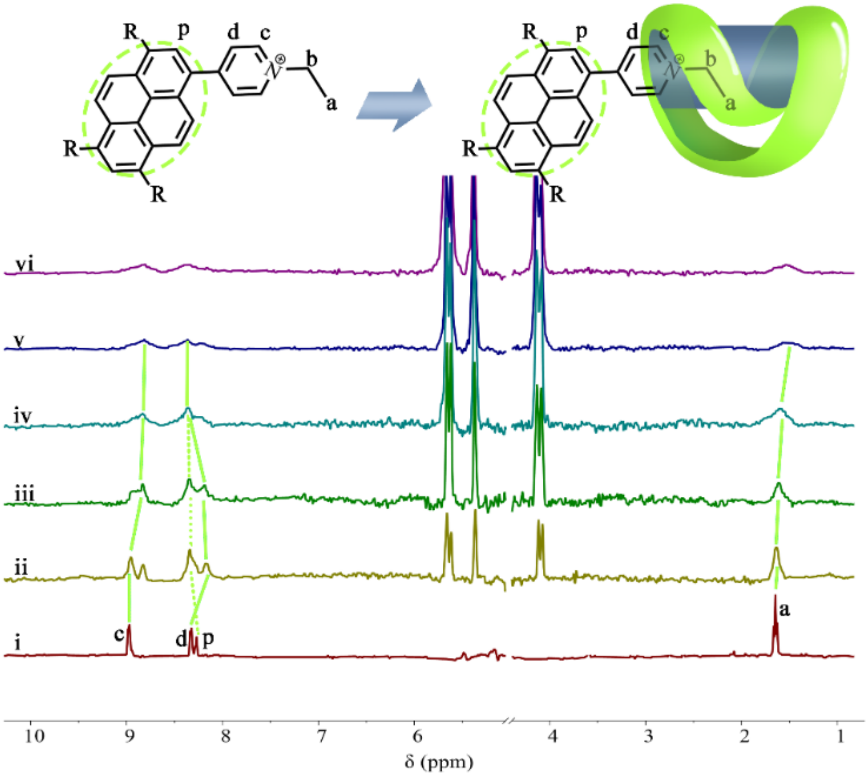

Figure 1. ^{1}H NMR titration spectra of **TPYP** (1 mM) on addition of different molar equivalents of ***t*Q[14]**: (i) free **TPYP**, (ii) 0.5, (iii) 1.00, (iv) 1.50, (v) 2.00, (vi) 2.50 recorded in D_2O at 25°C (R = *N*-ethylpyridinium bromide).

Fluorescence spectroscopy was used to further explore the molar ratio and interactions that accompany the changes in fluorescence, (Figures 2a and S6). Upon gradual addition of *t*Q[14], the emission intensity of TPYP at 490 nm gradually red-shifted to 485 nm in aqueous solution and its intensity steadily decreased with a well-defined balance point $N_{tQ[14]}$: N_{TPYP}=2:1. Moreover, the aqueous solution of TPYP-*t*Q[14] exhibited an obvious Tyndall effect (Figure 2a and the insert), and the aggregation was also observed under a confocal fluorescence microscope (Figure 2b and 2c). The scattered fluorescent spots gather into larger fluorescent spots, which reveals the initial formation of the supramolecular polymers TPYP-*t*Q[14]. The interaction mode of the polymer can be roughly summarized as: *t*Q[14] binds with the alkyl chain and pyridine parts of the TPYP in the molar ratio of 2:1 (*t*Q[14]:TPYP) via host-guest interactions.

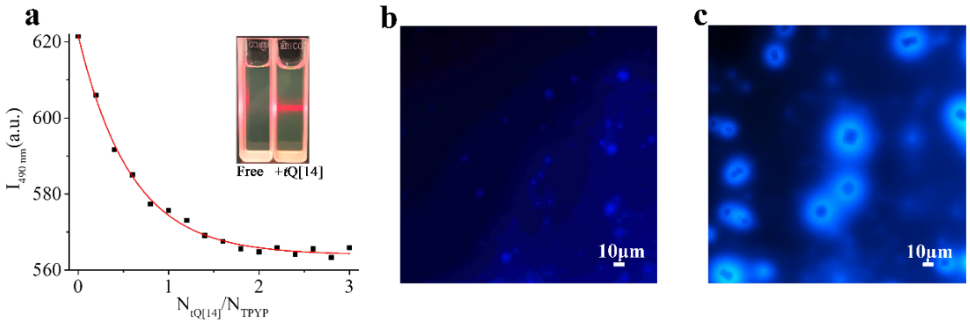

Figure 2. Fluorescence spectra of (a) **TPYP** (20 μM) upon addition of increasing concentrations of ***t*Q[14]** at λ_{max}=490 nm, pH=4.75 and insert: Tyndall effect of **TPYP** before and after binding with ***t*Q[14]**. The confocal microscopy images of (b) 20 μM **TPYP** and (c) 20 μM **TPYP-*t*Q[14]**.

To further confirm the formation of the supramolecular polymers, SEM experiments were conducted. As shown in Figures 3a and 3b, the supramolecular polymer TPYP-*t*Q[14] exhibits a loose and porous network structure under SEM which is attributed to the interaction between *t*Q[14] and TPYP in a ratio of 1:2. Meanwhile, the particle size of the TPYP in the presence of *t*Q[14] is greatly increased from 5.4 nm to 228.21 nm, indicating the aggregation caused by the host-guest interaction of TPYP-*t*Q[14] (Figure 3c). Then, the diffusion coefficient of TPYP was studied by the DOSY spectrum (Figure 3d), which revealed a downward trend from D_{TPYP} = 4.89×10^{-9} m^2s^{-2} to $D_{TPYP\text{-}tQ[14]}$= 2.59×10^{-9} m^2s^{-2} when *t*Q[14] was added, which means that the addition of *t*Q[14] slows down the diffusion of TPYP. All of the above experiments are consistent with the existence of porous and loose supramolecular polymer TPYP-*t*Q[14] constructed via host-guest interactions.

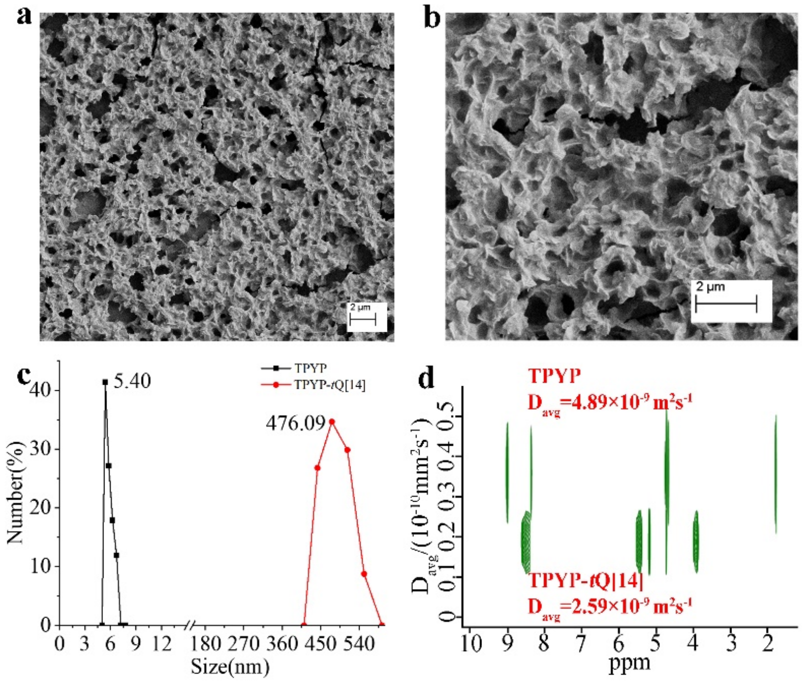

Figure 3. SEM images of **TPYP-*t*Q[14]** (a, b and scales are 2 *µ*m); DLS data of 20 µM **TPYP** (c, black) and 20 µM **TPYP-*t*Q[14]** (c, red); DOSY spectra of 1 mM **TPYP**(d, top) and 1 mM **TPYP-*t*Q[14]**(d, bottom).

Subsequently, to investigate the influence of metals on the polymer structure, a series of metal ions $M(ClO_4)_x$, M^{x+} for alkali, alkaline earth, lanthanide, Y^{2+}, Cr^{2+}, Mn^{2+}, Fe^{2+}, Fe^{3+}, Co^{2+}, Ni^{2+}, Cu^{2+}, Zn^{2+}, Cd^{2+}, Ag^{+}, Hg^{+}, and Al^{3+} were separately added. It was found that TPYP-*t*Q[14] shows good selectivity toward Ni^{2+} amongst the above ions, and that the fluorescent intensity of TPYP-*t*Q[14] in the presence of Ni^{2+} was also significantly reduced (Figures S7, S8). In addition, TPYP-*t*Q[14] also shows a high anti-interference ability in the presence of the other metal ions when detecting Ni^{2+} (Figure S9). To further explore the mechanism of TPYP-*t*Q[14] in the presence of Ni^{2+}, a fluorescence titration was carried out. As shown in Figure 4a, the fluorescent intensity of TPYP-*t*Q[14] continues to decrease from 573 a.u. to 125 a.u. with the addition of Ni^{2+}, and the corresponding detection limit is calculated at 1.54×10^{-7} M (Figure S10). Meanwhile, a precipitate with yellow-green emission was found at the bottom of the solution, which was not observed in the case of TPYP, *t*Q[14], or *t*Q[14]- Ni^{2+} individually (Figure S11).

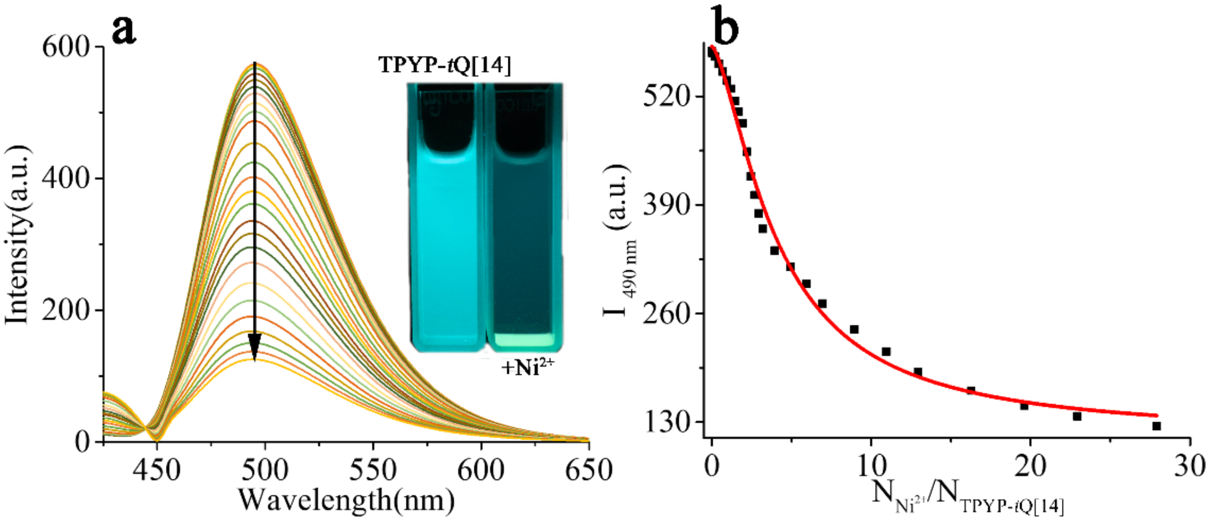

Figure 4. Fluorescence spectra (a) of 20 μM **TPYP-*t*Q[14]** upon addition of increasing concentrations of Ni^{2+}and the curve (b) of intensity *vs*. $N_{Ni}{}^{2+}/N_{TPYP\text{-}tQ[14]}$ at λ_{em}=490 nm.

NMR spectroscopy was used to investigate the reasons for the reduced fluorescence of the polymer and the corresponding precipitation. As shown in Figure 5d, the addition of nickel ions directly leads to the disappearance of the proton signals for TPYP-*t*Q[14], which means that the nickel ions induce the precipitation of the entire polymer rather than any single component of TPYP or *t*Q[14]. Therefore, it could be inferred that a metal-coordinated ternary supramolecular polymer TPYP-*t*Q[14]-Ni^{2+} is formed, and the interactions of TPYP-*t*Q[14]-Ni^{2+} involve classic coordination and host-guest interactions. The dominant host-guest interaction is still between TPYP and *t*Q[14] because the addition of Ni^{2+} into TPYP-*t*Q[14] makes both of their proton signals disappear. The dominant coordination interaction should be between Ni^{2+} and *t*Q[14] given the protonated TPYP has lost the ability of metal coordination [21]. At the same time, the *t*Q[14] has two relatively independent cavities and three metal coordination regions, and two of the cavities and the two coordination sites of the portal a and b (Scheme 1) are occupied due to the host-guest interaction of TPYP-*t*Q[14], while portal c is in an "idle" state. Thus, Ni^{2+} is able to coordinate with the portal c of *t*Q[14] from the perspective of ionic radius because the ionic radius of Ni^{2+} ions (0.69 pm) is smaller than Eu^{2+}(1.31 pm), Dy^{2+} (1.21 pm) and Cd^{2+} (0.92 pm) that could be coordinated with the portal c of *t*Q[14] reported previously [1]. UV-vis spectroscopy further verified the above inference. The absorption of TPYP-*t*Q[14] at $\lambda = 425$ nm increased on addition of Ni^{2+} accompanied by a blue-shift of about 27 nm (Figure S12), indicating that the Ni^{2+} is located at the portal c of the *t*Q[14], and influences the electron distribution of the included aromatic ring of TPYP and finally causes the π-π^* transition. Meanwhile, the morphology of the yellow precipitation of TPYP-*t*Q[14]-Ni^{2+} observed under SEM is verified in Figure 5a. Many ordered chain-like polymers are formed on addition of Ni^{2+} which is different from that of TPYP-*t*Q[14] (Figure S13). In general, the double cavities of *t*Q[14] tightly bind with the TPYP through host-guest interactions, while the portal c of *t*Q[14] coordinates with Ni^{2+} via a coordination interaction, resulting in the morphology of TPYP-*t*Q[14] changing from a loose and porous network to a straight chain-like polymer of TPYP-*t*Q[14]-Ni^{2+}.

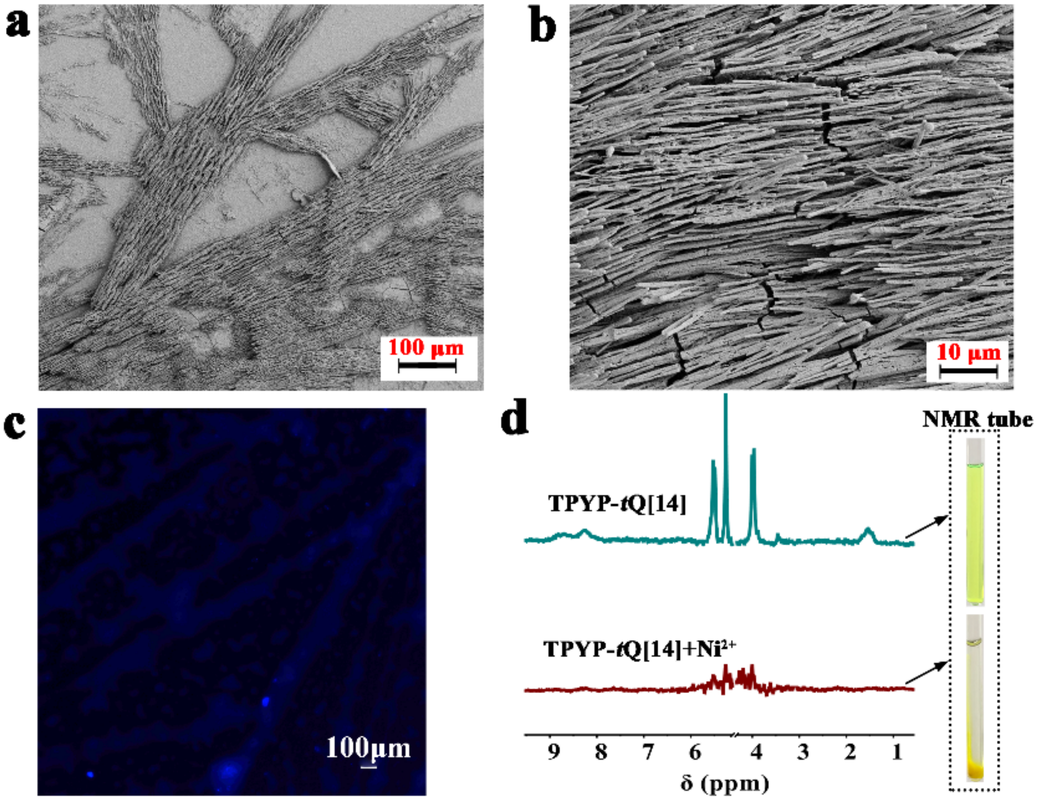

Figure 5. SEM images (a, b) of TPYP-*t*Q[14]-Ni^{2+}; The confocal microscopy images (b) of 20 μM TPYP-*t*Q[14]-Ni^{2+}; ^{1}H NMR spectra (d) of 1 mM TPYP-*t*Q[14] and 1 mM TPYP-*t*Q[14]-Ni^{2+}, and the corresponding insert is the NMR tube for TPYP-*t*Q[14] and in the presence of Ni^{2+}, respectively.

Conclusions

In conclusion, TPYP is specially designed for the preparation of *t*Q[14]-based supramolecular polymers. At the same time, ^{1}H NMR spectroscopy, fluorescence spectroscopy and other methods have been used to verify the interaction of TPYP-*t*Q[14]. *T*Q[14] binds with the pyridines and alkyl chains of TPYP, and extends around to form a loose and porous supramolecular polymer. Subsequently, the fluorescence intensity of TPYP-*t*Q[14] decreased sharply by adding Ni^{2+}. The Ni^{2+} coordinates with the portal c of *t*Q[14] and further regulates the structure of TPYP-*t*Q[14] from a loose porous structure to a chain-like TPYP-*t*Q[14]-Ni^{2+} polymer. This research makes full use of the third portal of the twisted cucurbit[14]uril, and provides a new method for controlling the structure of a polymer via a coordination interaction with a metal.

AUTHOR INFORMATION

Corresponding Author

* Xin Xiao (gyhxxiaoxin@163.com)

Present Addresses

[a] Key Laboratory of Macrocyclic and Supramolecular Chemistry of Guizhou Province, Guizhou University, Guiyang 550025, China

[b] Department of Chemistry, University of Hull, Hull HU6 7RX, U.K

Author Contributions

Yang Luo: Validation and writing - original draft

Wei Zhang: Resources

Mao Xia Yang: Data curation

Xian Hao Feng: Investigation

Carl Redshaw: Writing - review & editing

Qing Li: Supervision

Zhu Tao: Supervision

Xin Xiao: Carried out manuscript editing, conception, design of the study, formal analysis, revising it critically for intellectual content.

Supporting Information

Synthetic route, ^{1}H NMR/^{1}H-^{1}H COSY/Mass and fluorescence spectra of **TPYP**; ^{1}H NMR spectrum of **1**; Fluorescence spectra for **TPYP** + ***t*Q[14]**; Interference experiments including UV-vis spectroscopy.

Funding Sources

We thank the National Natural Science Foundation of China (NSFC No. 21861011, 21871064), the Innovation Program for High-level Talents of Guizhou Province (No. 2016-5657) and Graduate scientific research Fund of Guizhou Province (No. YJSKYJJ[2021]021) are gratefully acknowledged for financial support. CR thanks the EPSRC for an Overseas Travel Grant (EP/R023816/1).

REFERENCES

[1] Cheng, X. -J.; Liang, L. L.; Chen, K.; Ji, N. -N.; Xiao X.; Zhang, J. -X.; Zhang, Y. -Q.; Xue, S. -F. Zhu, Q. -J.; Ni, X. -L.; Tao, Z. Twisted Cucurbit[14]uril. *Angew. Chem. Int. Ed.* **2013**, *52*, 7252-7255.

[2] Day A. I.; Arnold A. P.; Blanch R. J. (Unisearch Limited, Australia), PCT Int. Appl. 2000, WO2000 - 2000AU412 20000505, 112 (Priority: AU 99 - 232 19990507).

[3] Kim, J.; Jung, I. -S.; Kim, S. -Y.; Lee, E.; Kang, J. -K.; Sakamoto, S.; Yamaguchi, K.; Kim, K. New Cucurbituril Homologues: Syntheses, Isolation, Characterization, and X-ray Crystal Structures of Cucurbit[*n*]uril (n = 5, 7, and 8). *J. Am. Chem. Soc.* **2000**, *122*, 540-541.

[4] Zhang, J.; Tang, Q.; Gao, Z. -Z.; Huang, Y.; Xiao, X.; Tao Z. Stimuli-Responsive Supramolecular Assemblies between Twisted Cucurbit[14]uril and Hemicyanine Dyes and Their Analysis Application. *J. Phys. Chem. B*. **2017**, *121*, 11119-11123.

[5] Zhang, J.; Xi, Y. -Y.; Li, Q.; Tang, Q.; Wang, R.; Huang, Y.; Tao Z.; Xue, S. -F.; Lindoy, L.; Wei, G. Lindoy, L. F.; Wei, G. Supramolecular Recognition of Amino Acids by Twisted Cucurbit[14]uril. *Chem. Asian J*. **2016**, *11*, 2250-2254.

[6] Li, Q.; Qiu, S. -C.; Chen, K.; Zhang, Y.; Wang, R.; Huang, Y.; Tao, Z.; Zhu, Q. -J.; Liu J. -X. Encapsulation of alkyldiammonium ions within two different cavities of twisted cucurbit[14]uril. *Chem. Commun*. **2016**, *52*, 2589.

[7] Liu, Q.; Li, Q.; Cheng, X. -J.; Xi, Y. -Y.; Xiao, B.; Xiao, X.; Tang, Q.; Huang, Y.; Tao, Z.; Xue, S. -F.; Zhu, Q. -J.; Zhang, J. -X. A novel shell-like supramolecular assembly of 4,4'-bipyridyl derivatives and a twisted cucurbit[14]uril molecule. *Chem. Commun*. **2015**, *51*, 9999-10001.

[8] Wang, C. -H.; Tang Q.; Zhang, J.; Yao, Y. -Q.; Xiao, X.; Huang, Y.; Tao Z. Alkaline earth cation-mediated photoluminescent complexes of thioflavin T with twisted cucurbit[14]uril. *New J. Chem*. **2018**, *42*, 9244-9251.

[9] Gao, Z.; Zhang, J.; Sun, N.; Huang, Y.; Tao, Z.; Xiao, X.; Jiang J. Hyperbranched supramolecular polymer constructed from twisted cucurbit[14]uril and porphyrin via host-guest interactions. *Org. Chem. Front*. ***2016***, 3, 1144-1148.

[10] Yang, Y.; Ni, X. -L.; Xu, J. -F.; Zhang X. Fabrication of nor-seco-cucurbit[10]uril based supramolecular polymers via self-sorting. *Chem. Commun*. **2019**, *55,* 13836-13839.

[11] Babu, S. S.; Praveen, V. K.; Ajayaghosh A. Functional π-Gelators and Their Applications. *Chem. Rev.* **2014**, *114*, 1973-2129.

[12] Gao, R. H.; Chen, L. X.; Chen, K.; Tao, Z.; Xiao X. Development of hydroxylated cucurbit[*n*]urils, their derivatives and potential applications. *Coordin. Chem. Rev.* **2017**, *348*, 1-24.

[13] Liu, M.; Kan, J.; Yao, Y.; Zhang, Y.; Bian, B.; Tao, Z.; Zhu, Q.; Xiao X. Facile preparation and application of luminescent cucurbit[10]uril-based porous supramolecular frameworks. *Sensor Actuat B: Chem.* **2019**, *283*, 290-297.

[14] Yu, G.; Jie, K.; Huang F. Supramolecular Amphiphiles Based on Host-Guest Molecular Recognition Motifs. *Chem. Rev.* **2015**, *115*, 7240-7303.

[15] Ogoshi, T.; Kakuta, T.; Yamagishi, T. -A. Applications of Pillar[*n*]arene-Based Supramolecular Assemblies. *Angew. Chem. Int. Ed.* **2019**, *58*, 2197 - 2206.

[16] Ni, X. -L.; Chen, S.; Yang, Y.; Tao, Z. Facile Cucurbit[8]uril-Based Supramolecular Approach To Fabricate Tunable Luminescent Materials in Aqueous Solution. *J. Am. Chem. Soc.* **2016**, *138*, 6177-6183.

[17] Yang, Y.; Ni, X. -L.; Xu, J. -F.; Zhang, X. Fabrication of nor-seco-cucurbit[10]uril based supramolecular polymers via self-sorting. *Chem. Commun.* **2019**, *55*, 13836-13839.

[18] Chen, X. -M.; Chen, Y.; Yu, Q.; Gu, B. -H.; Liu, Y. Supramolecular Assemblies with Near-Infrared Emission Mediated in Two Stages by Cucurbituril and Amphiphilic Calixarene for Lysosome-Targeted Cell Imaging. *Angew. Chem. Int. Ed.* **2018**, *57*, 12519-12523.

[19] Yang, L.; Tan, X.; Wang, Z.; Zhang, X. Supramolecular Polymers: Historical Development, Preparation, Characterization, and Functions. *Chem. Rev.* **2015**, *115*, 7196-7239.

[20] Sun, Y.; Guo, F.; Zuo, T.; Hua, J.; Diao, G. Stimulus-responsive light-harvesting complexes based on the pillararene-induced co-assembly of b-carotene and chlorophyll. *Nat Commun*. **2016**, *7*, 12042.

[21] Yang, Z.; Wang, Y.; Liu X. Vanderlinden, R. T.; Ni, R.; Li, X.; Stang, P.J. Hierarchical Self-Assembly of a Pyrene-Based Discrete Organoplatinum(II) Double-Metallacycle with Triflate Anions via Hydrogen Bonding and Its Tunable Fluorescence Emission. *J. Am. Chem. Soc*. **2020,** *142*, 13689-13694.

[22] Zhao, Z.; Chen, S.; Lam, J. W. y.; Lu, P.; Zhong, Y.; Wong, K. S.; Kwok, H. S.; Tang, B. Z. Creation of highly efficient solid emitter by decorating pyrene core with AIE-active tetraphenylethene peripheries. *Chem. Commun*. **2010**, *46*, 2221-2223.

[23] Figueira-Duarte, T. M.; Müllen, K. Pyrene-Based Materials for Organic Electronics. *Chem. Rev*. **2011**, *111*, 7260-7314.

[24] Hagiwara, S.; Ishida, Y.; Masui, D.; Shimada, T.; Takagi, S. Unique Photochemical Behavior of Novel Tetracationic Pyrene Derivative on the Clay Surface. *Tetrahedron Lett*. **2012**, *53*, 5800-5802.

[25] Chan, K. L.; Lim, J. P. F.; Yang, X.; Dodabalapur, A.; Jabbour, G. E. High efficiency pyrene-based blue light emitting diodes: aggregation suppression using a calixarene 3D-scaffold. *Chem. Commun*. **2012**, *48*, 5106-5108.

[26] Mei, J.; Leung, N. L. C.; Kwok, R. T. K.; Lam, J. W. Y.; Tang, B. Z. Aggregation-Induced Emission: Together We Shine, United We Soar!. *Chem. Rev.* **2015**, *115*, 11718-11940.

[27] Mako, T. L.; Racicot, J. M.; Levine, M. Supramolecular Luminescent Sensors. *Chem. Rev.* **2019**, *119*, 322-477.

[28] Ni, Y.; Song, J.; Wang, F.; Kan, L.; Song, J.; Wang, W.; Ma, W.; Zhang, W.; He, G. Pyrenoviologen-based Fluorescent Sensor for Detection of Picric Acid in Aqueous Solution. *Chinese Chemical Letters*. **2019**, *30*, 1984-1988.

[29] Guo, B. -B.; Lin, Y. -J.; Jin, G. -X. Controllable Construction of Half-sandwich Octanuclear Complexes Based on Pyridylsubstituted Ligands with Conjugated Centers. *Dalton Trans.* **2017**, *46*, 8190.

[30] Aitchison, C. M.; Kane, C. M.; McMahon, D. p.; Spackman, P. R.; Pulidpo, A.; Wang, X.; Wilbraham, L.; Chen, L.; Clowes, R.; Zwijnenburg, M. A.; Sprick, R. S.; Little, M. A.; Day, G. M.; Cooper, A. I. Photocatalytic Proton Reduction by A Computationally Identified, Molecular Hydrogenbonded Framework. *J. Mater. Chem. A*. **2020**, *8*, 7158-7170.

[31] Ni, X. L.; Xiao, X.; Cong, H.; Zhu, Q.; Xue, S.; Tao, Z. Self-Assemblies Based on the "Outer-Surface Interactions" of Cucurbit[*n*]urils: New Opportunities for Supramolecular Architectures and Materials. *Acc. Chem. Res.* **2014**, *47*, 1386-13.

[32] Huang, Y.; Gao, R. -H.; Liu, M.; Chen, L. -X.; Ni, X. -L.; Xiao, X.; Cong, H.; Zhu, Q. -J.; Chen, K.; Tao, Z. Cucurbit[*n*]uril-Based Supramolecular Frameworks Assembled through Outer-Surface Interactions. *Angew. Chem. Int. Ed.* **2021**, *60*, 15166-15191.